Numerical Simulation of Impact Welding Processes with LS-DYNA

Peter Groche[1], Christian Pabst[1]

[1]Institute for Production Engineering and Forming Machines, Technische Universität Darmstadt

1 Abstract

Impact welding enables metallurgical bonding even between dissimilar metals. The bond is formed during a high speed impact between the two workpieces to be joined under accurately defined conditions. In the application, the accelerating force is provided by an explosive (explosion welding, EXW) or by an electromagnetic field (electromagnetic pulse welding, EMPW). One workpiece is usually accelerated within a few millimeters up to 200 m/s and above. The impact and consequently the bond formation takes place in only a few microseconds which makes it hard to observe. In order to enable the observation of the two mentioned processes, a test rig has been built at the Institute for Production Engineering and Forming Machines which produces the impact purely mechanically.
The numerical simulation with LS-DYNA is used to gain detailed insights into the process. Three phenomena, which are thought to have a significant effect on the bond formation, are currently investigated numerically: The supersonic displacement of the surrounding gaseous medium, the strains and strain rates at the bonding zone and the macroscopic flow of material.
The results of the numerical simulations are compared to experimental and metallographic investigations. The comparison and fusion of the findings are used to draw new conclusions on the formation mechanisms of the bonding zone.

2 Impact welding: process principles

Impact welding has been accidentally observed first during the First World War. It was found that projectiles were bonded to armor [1]. The first application was explosion welding, which also utilizes explosives to accelerate one workpiece towards the other. The high energy of explosives enables joining even large plates with a thickness of several millimeters which is why the process is also called explosion cladding. A distinction is made between the accelerated workpiece (the flyer) and the stationary workpiece (the target or backer). The thickness of the latter can reach several centimeters because it does not need to be accelerated. One important application is the production of containers for the chemical industry. The ability of joining large plates is a great advantage, but handling explosives is very dangerous and the preparation takes a lot of time. [2]
In the late 60s and early 70s, electromagnetic pulse welding has been developed [3,4]. Instead of explosives, this process draws the accelerating force on the flyer from a strong pulsed electromagnetic field. A strong alternating current is driven through the nearby so-called tool coil which creates this field. Corresponding to Lenz's rule, both the eddy current in the flyer and the current in the coil flow in opposite directions and thus repel each other (Lorentz force). The current for the coil is provided by charged high voltage capacitors. Together with the coil, they form a damped oscillating circuit. For most welding processes, only the first half-wave of the current is important. The impact takes place within this period and the weld is completed. The charging voltage can reach several ten kilovolts, the energy of the capacitors can be more than 100 kilojoules and the peak current of the first oscillation can exceed one mega ampere. The discharge frequency strongly depends on the inductance and the capacity of the whole circuit and can reach from only a few to a hundred kilohertz. This means that the first half-wave only takes a few microseconds. Within this period, the flyer is accelerated and impacts the target. In contrast to explosion welding, the available energy from the capacitors is much lower and thus only allows for much smaller weld areas. However, the great advantage is its industrial applicability: The charging time is in the range of only a few seconds and the lifetime of the equipment enables mass production. [5,6,7]
Despite the great advantages especially of electromagnetic pulse welding, a wide spread is still hindered by a poor process understanding. The governing mechanisms and their influencing factors are not fully understood yet. Consequently, the design of the joint and the tool is still performed largely empirically.
Impact welding basically requires a collision between two workpices at a certain angle (β_{imp}) and at a certain velocity (v_{imp}), as indicated in figure 1. The closing gap is always necessary to obtain a weld.

The impact velocity is usually in the range of several hundred meters per second, the angle is in the range of ten degrees and above.

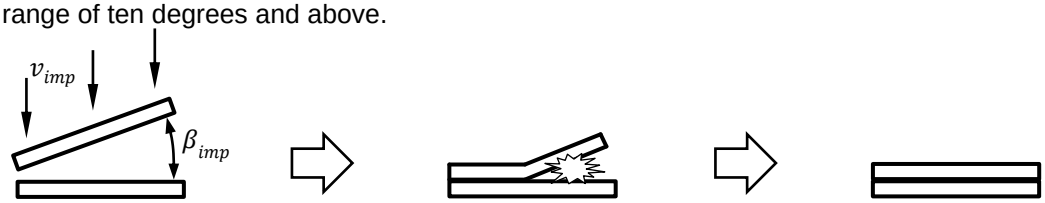

Fig.1: Schematic illustration of an impact welding process.[8]

Figure 2 illustrates important values at the collision point (left) and a schematic process window (right). From explosion welding, which is the older process, it is known that the angle at the collision point and its velocity (often denoted β and v_c) determine the process window [1,2,9,10]. It must be noted that the macroscopic values of the impact, v_{imp} and β_{imp}, do not usually correspond to the microscopic values β and v_c. They have to be in a certain range to allow for a bond, which is shown in the process window. It depends on the material combination to be joined, other influencing factors are not regarded. The process window may be a helpful tool, but does unfortunately not explain the very basic process mechanisms.

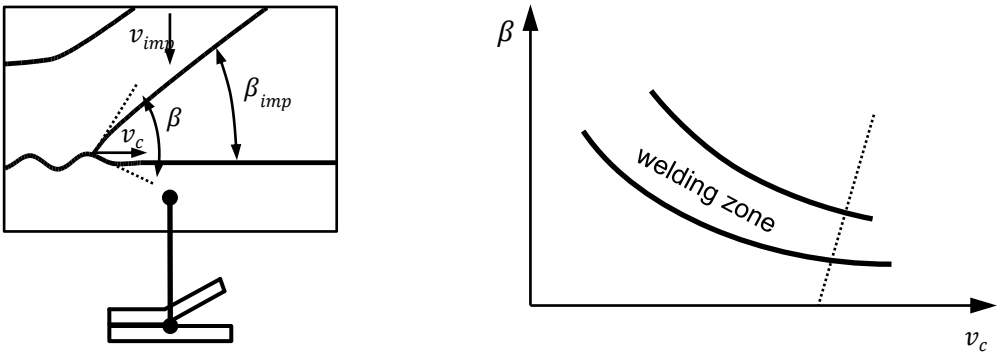

Fig.2: Typical impact geometry (left) and schematic process window (right).[11]

One important phenomenon in impact welding is “jetting” which occurs during the impact and helps cleaning the surfaces. Superficial layers of contaminants and oxides are expelled from the closing gap. This material forms the so-called jet, a flow of solid material whose composition varies for example depending on the hardness of the materials of the sheets. Detailed experimental and numerical investigations have been performed in [12,13]. The dotted line in the process window in figure 2 indicates a barrier after which jetting is not possible any more. This is usually the speed of sound in the material. If the collision point travels faster, i.e. the gap closes faster, the jet cannot escape and is trapped in the joint area where it prohibits the weld. Thus jetting is known to be crucial for the process [10].
During the impact, a bright flash between the colliding workpieces can be observed as another phenomenon [8]. The origin of this light emission and its role during the bond formation has not been investigated yet, although it might be closely associated.
Although the mechanisms in explosion welding and in electromagnetic pulse welding are likely to be identical, the processes have one great difference: In explosion welding, angle and velocity are quite constant during the weld formation, whereas both constantly change in electromagnetic pulse welding. Consequently, during the impact, both parameters cross the process window and a characteristic line-shaped joint area is created.

3 Impact welding: theory of the bond formation

Impact welding is thought to be a cold joining process which does not produce any heat in the parts to be joined [14]. However, studies from the recent years have shown that the joint area always exhibits a very thin interlayer [15,16]. In case of similar metals it consists of ultra fine grains [17], in case of dissimilar metals intermetallic phases can be found [16,17,18]. As the thickness of this interlayer is in the region of nanometers or only few micrometers, its negative influence on the joint strength is usually negligible.
Based on these findings, the authors have developed a new hypothesis. It implies that the interlayer is caused by a quick melting and solidification process [8]. This theory is supported by the light emission

during the impact which might indicate the presence of high temperatures. During the impact and during the closing of the gap between the workpieces, the surrounding gas is ejected from the gap at supersonic speeds. This fast compression could lead to a rapid increase in temperature which could be sufficient to melt a thin superficial layer of the workpieces, creating a thin fusion weld. Earlier investigations have shown that the brightness of the light emission during the impact depends on the composition of the surrounding media [8]. An analytical estimation of the temperatures during the supersonic compression for different gases has been performed in [19]. The results show that the temperature reaches from about 900 K to several thousand Kelvin, which could be enough to melt metal surfaces.
Furthermore, the following issues will be treated in this paper to enable the numerical prediction of the impact welding process in the future:

- Does the transient behavior of electromagnetic pulse welding influence the process window? Is a weld immediately created when angle and velocity reach the process window?
- How big is the influence of the material model on the results? Are there other influencing factors on the result which derive solely from the numerical simulation?

The first question will be answered by experimental investigations compared to numerical results. If the impact conditions remain constant according to the simulation but the properties of the welded area change, a transient behavior can be assumed. If the appearance of the weld can be explained with simultaneous changes in the impact conditions, a close correlation is plausible.
The second question will be answered by the comparison of numerically and experimentally welded specimen. If the material flow is predicted correctly, the geometries after the weld should be almost identical.

4 Experimental setup: test rig

In section 2 it has been shown that the two industrially available impact welding processes have great disadvantages when it comes to their observability. In order to avoid these limitations, a test rig has been developed at the Institute for Production Engineering and Forming Machines. It utilizes neither explosives nor electromagnetic fields but mechanical force to accelerate the specimens. It mainly consists of two rotors with one specimen attached to one end of one rotor each. The test rig makes them collide in the centre with twice the speed. Figure 3 shows the physical setup (left) and a schematic drawing of the working principle. The black background and the black rotors are important for high speed imaging.

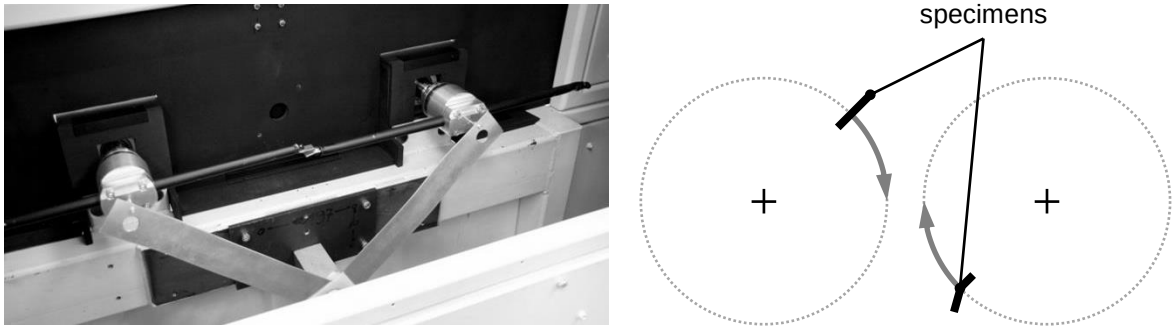

Fig.3: Photograph of the two rotors of the test rig inside the housing (left), schematic drawing of the setup (right).

With a diameter of 500 mm and a maximum speed of 6000 rpm, each specimen can be accelerated theoretically to about 150 m/s, adding up to about 300 m/s when both specimen collide. So far, the maximum velocity is limited to 125 m/s (5000 m/s) due to stability issues concerning the control of the motors. The setup allows the impact velocity and the impact angle to be adjusted independently. Figure 4 shows the installed samples on the left side and the joined samples on the right side. One part of each sample is bolted to a specimen fixture. Once the weld is established, each sample breaks into two parts, which is enabled by a breaking point and the hardened, sharp-edged specimen fixtures made of tool steel. The specimens are made of commercially pure aluminum (EN AW1050A or AL99.5) with a thickness of 2 mm.

Fig.4: Detailed photograph of two specimens in collision position, the adjusted angle is 15° and the impact surface is 12x12 mm each (left). Welded specimens separated from the clamped part (right, [11])

The joined specimen is welded homogeneously almost along almost the whole length, as can be seen from the micrograph in figure 5. The wavelength of approximately 25 µm is almost constant along the cross section. The experiment has been carried out with an impact velocity of 250 m/s (5000 rpm for each rotor) and an impact angle of 10°.

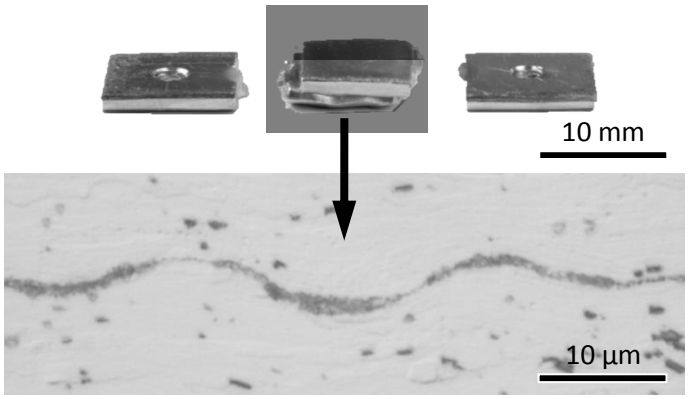

Fig.5: Microscopic view of the joint area between two specimens from the test rig [11].

5 Experimental setup: electromagnetic pulse welding

The welding trials are carried out using a standard sheet metal welding tool coil and a pulse generator from PSTproducts. The pulse generator delivers a maximum energy of 32 kJ at a maximum charging voltage of 16 kV. The current is concentrated in the coil and driven through the effective part with a square cross section of 5 x 5 mm. The oscillating circuit consisting of coil and pulse generator (i.e. cables and capacitors) has a natural frequency of 20 kHz, the maximum peak current of the first half wave is above 400 kA. For the experiment and the simulation the discharge current is set to 300 kA.
A simple standard sheet metal welding geometry is used for the experiments, which is shown in figure 6. The sheets are made of the same batch with a thickness of 2 mm as for the test rig's experiments (EN AW1050A). They have a size of 50 x 50 mm and the initial distance is 2 mm. The coil is separated from the target sheet by a thin insulating layer (0.7 mm). The target sheet is supported by a block of steel to prevent it from moving by the impulse from the impact. The photograph of a welded specimen is depicted in figure 6 as well. It can be seen that only the central part below the coil has been moved. The joint area can be found here. Its main characteristic is the o-shaped welding seam [20]. Both sheets are kept in place with the help of spacers (not shown here), but they are neither necessary for the real process nor for the simulation. Due to the high acceleration, the mass alone is sufficient to keep the surrounding material in place.

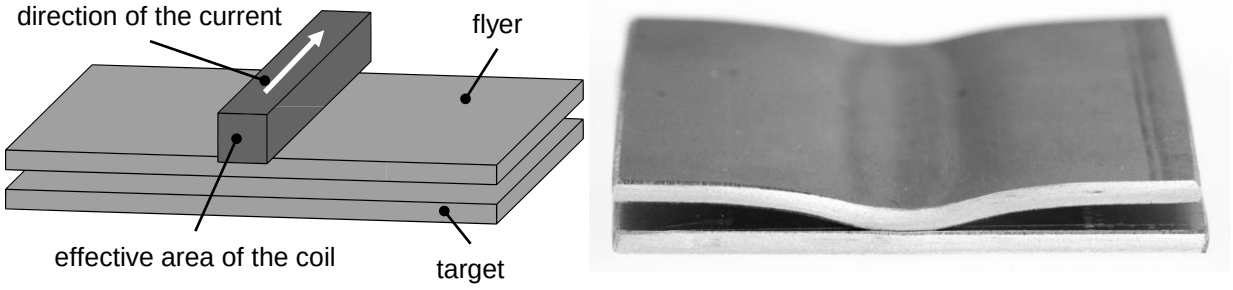

Fig.6: Schematic representation of a simple setup for electromagnetic sheet metal pulse welding (left) and photograph of a joined specimen (right).

6 Numerical simulation of the impact

Two methods of welding by a high speed impact have been presented: Electromagnetic pulse welding and welding with the help of the test rig. In order to get information about the conditions in the joining area, numerical simulations are carried out. The simulation is not intended to represent microscopic effects, these investigations have been performed by other researchers yet [21]. The aim is to evaluate angle and velocity at the collision point, relying on the past findings in explosion welding which have been described in section 2.
The process of the test rig is simplified and reduced to a setup with two plates in two dimensions, depicted in figure 7. Their thickness is 2 mm to match the experiments and the length is 10 mm. Possible effects of the breaking points of each specimen have not been taken into account here. As initial condition, a velocity of 125 m/s each is chosen to match the experiments from section 4. The mesh size and element distribution has not been optimized for this simulation, but does not greatly affect the development of the process window. The element size is 0.1 x 0.1 mm.

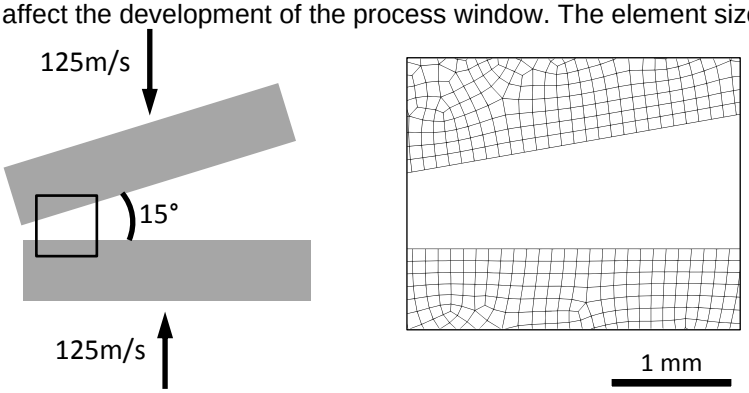

Fig.7: Geometry and mesh for the simplified test rig setup.

For electromagnetic pulse welding, the model is a one-to-one copy of the setup described in section 5. The coil overlaps the sheets by 5 mm at both ends, because the electromagnetic field is very inhomogeneous close to input and output faces in the numerical simulation. The sheet thickness is 2 mm as well as the distance. Figure 8 shows the geometry and the mesh size.

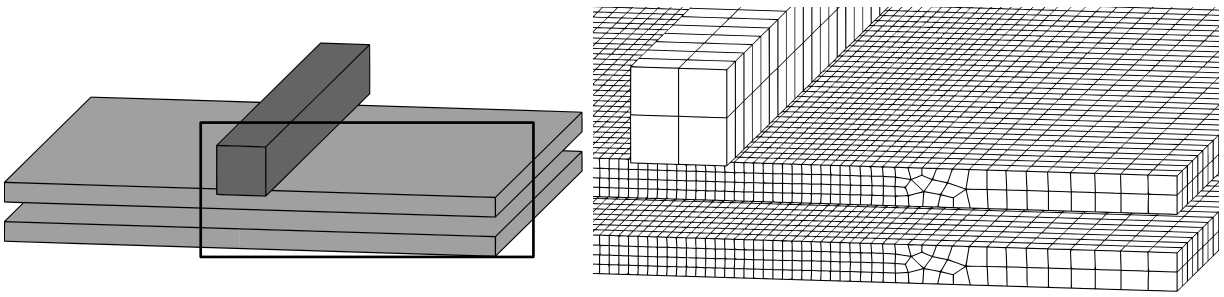

Fig.8: Geometry and mesh for the electromagnetic pulse welding setup.

The mesh size is largely dominated by the demands of the electromagnetic solver. The propagation of the electromagnetic field is calculated using boundary elements. A sensible reduction of elements consequently reduces significantly calculation time and memory usage. The following considerations have been made:

- Only the coil and the flyer are calculated by the EM solver. The target is treated as insulator. This is possible because the electromagnetic field is almost completely shielded by the flyer. Other applications with a much greater target are likely to require the target to be taken into account.
- The outer areas of the flyer are not important for the mechanical solver because they do not move, as described in the previous section 5. However, these regions are needed for the electromagnetic induction and the eddy currents inside the flyer. A coarse mesh is sufficient here.
- This simulation focuses on the impact which occurs first in the centre beneath the coil and then moves transversally to the coil. This is why the edge length of the elements in longitudinal direction of the coil is greater than in perpendicular direction.

The coil is not relevant here and thus modelled as a rigid body. The propagation of the electromagnetic field is barely influenced of the mesh size.
The current through the coil is given by a load curve. The values derive from real experiments and the amplitude is scaled according to the experiments to 300 kA. Figure 9 shows exemplarily the discharge

current of a typical electromagnetic pulse setup. The whole oscillation lasts for far less than a millisecond. As mentioned earlier, the process is usually finished during the first half wave within only few microseconds.

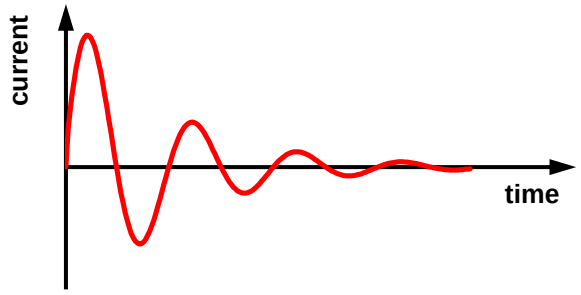

Fig.9: Discharge current versus time of a typical electromagnetic pulse application.

The electric conductivity of both flyer and coil is set constant and does not depend on the temperature for the simulation. This simplification does barely have an effect on the results. The matrices for the electromagnetic solver are recomputed every two electromagnetic time steps. The latter are automatically calculated by the solver. All other cards are identical for both the test rig setup and the electromagnetic pulse welding setup. The contact is always an automatic contact between surfaces, and a weld is simulated by a tiebreak contact. Elements of type 2 are used for all solid parts and shell elements of type 13 are used for the two-dimensional simulation. The material model by Johnson and Cook [22], *MAT_098 is utilized for both flyer and target. The parameters are taken from [23].

$$\sigma = (A + B\epsilon^n)(1 + C\ ln(\dot{\epsilon})) \quad (1)$$

A	B	n	C
140 MPa	75.2 MPa	0.6474	0.0125

Table 1: Parameters used for the material model by Johnson and Cook.

The set of process parameters for both the test rig setup and the electromagnetic pulse welding setup (i.e. velocity, angle and current) have been chosen because they allowed for a successful weld in both cases. It has been shown that the interfaces almost look identical for both setups [11].
The coordinates of all superficial nodes are written for each time step by LS-DYNA. The impact conditions are then evaluated using a custom script in Matlab. For each time step, the algorithm checks whether the surfaces are in contact, i.e. whether the distance between them falls below a given threshold value. In that case, angle and velocity at this point are calculated from the coordinates and the time vector and marked as point in the v_c-β diagram.

7 Discussion of the results

Figure 10 shows the results from the algorithm for both the electromagnetic pulse welding setup and the simplified test rig setup. As suspected in section 2, the impact parameters for electromagnetic pulse welding steadily change during the impact. The coordinates indicate where the corresponding values have been taken from the simulation. Figure 11 shows the location of the coordinates. The impact starts with a low angle but high collision point velocity. This is plausible because the angle is theoretically zero at the very first contact between flyer and target, as shown in figure 11 for this time step. Regarding the schematic process window in figure 2, no weld is possible here. This is proved by the microscopic images in figure 12. While the collision zone is travelling along the surface, its velocity continuously decreases until it comes to a stop. The resultant geometry depicted in figure 14 shows that the final angle is in the same order of magnitude. Regarding the microscopic images in figure 11, the weld is located between 1.5 mm and 3.7 mm from the centre.
The red points derive from the impact of the test rig geometry. Their position is roughly identical to where the joint area of the electromagnetic pulse welded sample is located. It is not helpful to connect the points by a line here as well, because their position in the diagram is not correlated to a position on the surface. The extension of the point is mainly determined by the element length and the settings of the analysing script. The coarser the mesh and the smaller the algorithm's tolerances, the more scattered are the points. In [11] it has been shown that the welded areas for both processes have a very similar appearance.

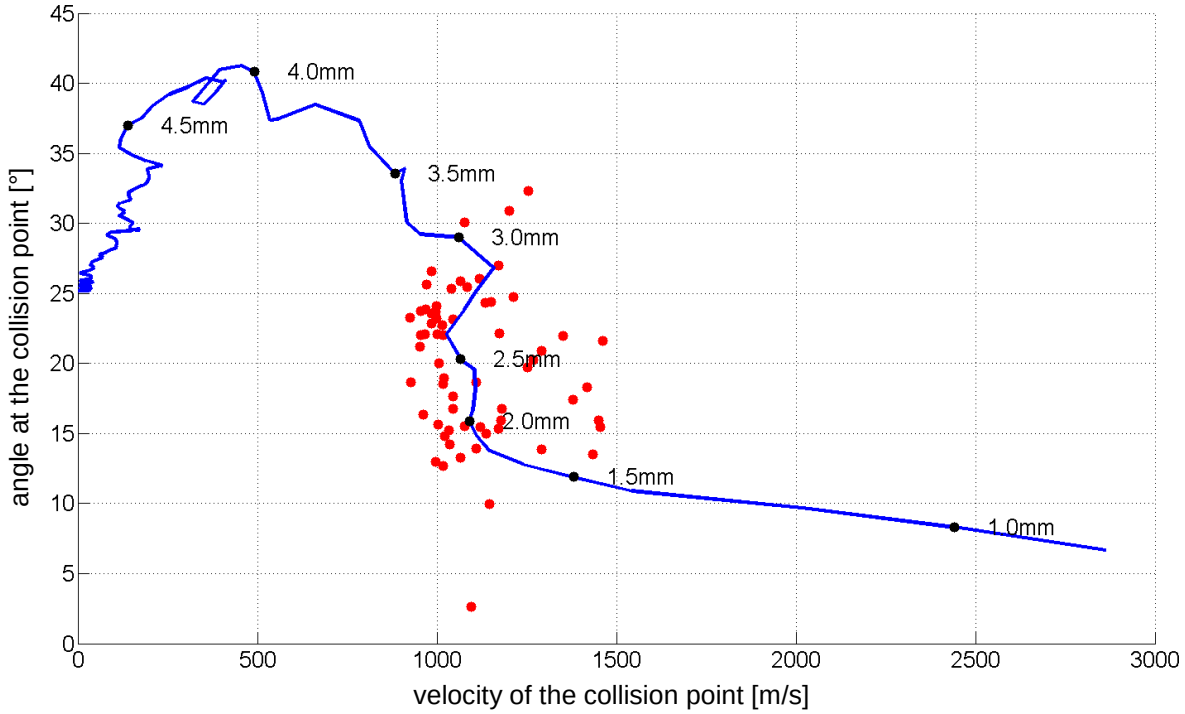

Fig.10: Angle and velocity at the collision point for electromagnetic pulse welding (blue line) and for the test rig simulation (red points). [11]

Fig.11: Cut view through the welding setup at the moment of the first contact between flyer and target.

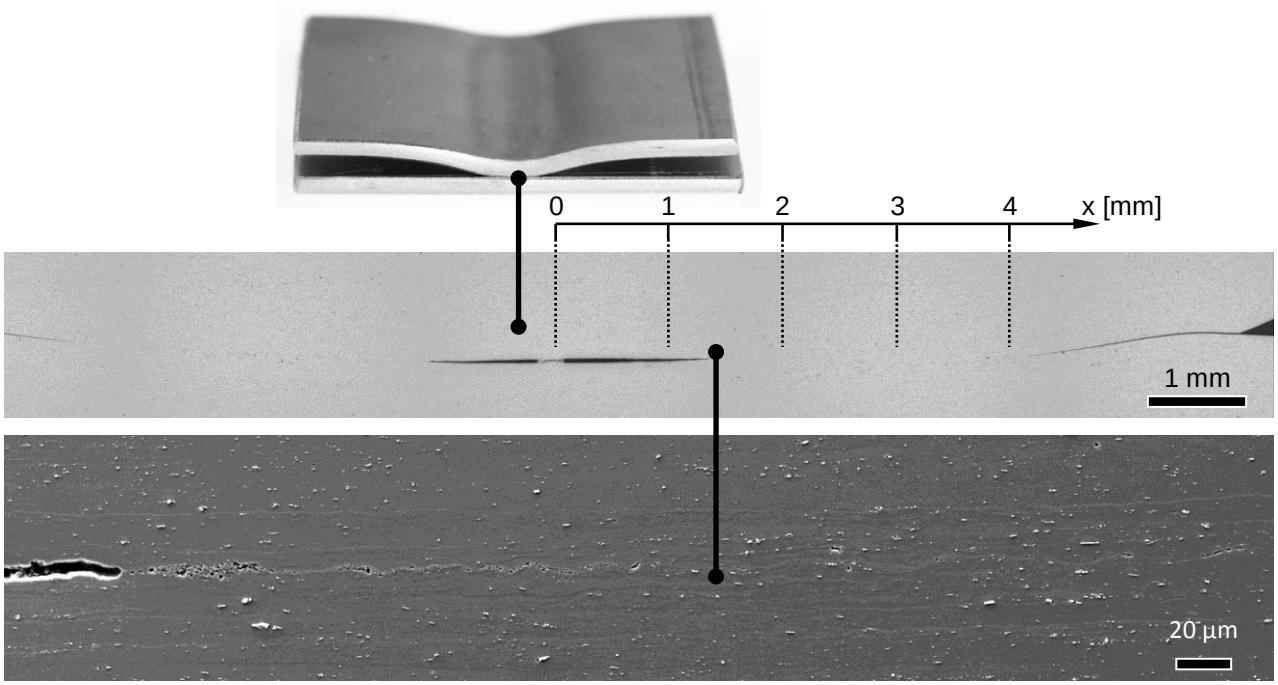

Fig.12: Position of the coordinates introduced for the process window diagram (top) and the initiation of the joint (bottom). [11]

For both electromagnetic pulse welding and the test rig experiments, no detailed high speed images exist from the impact so far to verify the simulation. Thus the only currently feasible method to compare simulation and experiment is the geometry after the impact. This is only possible with the electromagnetic pulse welded specimen and the corresponding simulations, because only here

macroscopic deformations can be observed after the process. Figure 13 shows the comparison between the cross sections of the experimentally welded specimen (compare figure 6 right) and the numerical result derived from the simulation. The maximum peak current is again 300 kA for both.

Fig.13: Comparison between the cross-sections of the numerical result (white) and the experimental result (red line).

The comparison shows that the numerical result is in satisfactory accordance with the experimental deformation. However, two major deviations can be identified: The height of the impact area in the center, where the two sheets are in contact and welded, is 0.2 mm less in the numerical simulation than in the experiment. The total width of the deformed area is about 4 mm less in the numerical simulation than in the experiment. Both observations lead to the conclusion that the numerical material model seems to be too soft. One possible reason is that the effect of strain rate hardening is not taken sufficiently into account.
Similar phenomena have been observed in [23]. The given parameters for the Johnson-Cook model are only valid for strain rates up to 10^3 1/s. However, during the acceleration of the flyer sheet, it experiences strain rates of more than $5 \cdot 10^4$ 1/s. As a solution, a modified material model is proposed in [23] which still bases on Johnson's and Cook's model but is more strain rate sensitive.
For a rough estimate, parameter C is increased from 0.0125 (table 1) to 0.05. In figure 14 the cross sections of resultant geometry is again compared to the cross section of the experimental result. Using the intersection of the two cross sections as quality criterion, the accuracy of the numerical simulation increased by more than 75%. Thus it can be concluded that the strain rate sensitivity is an important issue for material modelling in impact welding.

Fig.14: Comparison between the cross-sections of the numerical result with increased strain rate sensitivity (white) and the experimental result (red line).

8 Future works

One important task for future investigations is the adiabatic compression of the gas during the impact when the gap between the workpieces closes. The effect of different gases has been shown already in [8] and [19], but the influence on the joining process still remains unclear. Experiments with different gases will be carried out as a reference. The most important setup will enable welding in vacuum. If the theory of compression and heating is correct, this should make a weld impossible or at least have a significantly negative influence.
Further numerical work has to be done concerning the breaking point of the test rig specimens. It is necessary to make sure that it does not have any significant influence on the joining process. If this should be the case, it is crucial to quantify this influence to enable the comparison between electromagnetic pulse welding and the test rig. Furthermore, the results will show whether the transient character of the impact as shown in section 4 is caused by the process or by the influence of the breaking points.
The material modelling still requires improvement. The difference between the experiments and the numerical simulation complicates drawing the right conclusions. Other material models, which are valid for higher strain rates as the Jonson-Cook model, will be regarded in future investigations. Another aspect is the increasing influence of the material density as strain rates increase. During the acceleration of the flyer, it experiences more than 10^8 m/s^2. In addition, it is planned to use a ring expansion test to evaluate different material models.

9 Summary

Explosion welding and electromagnetic pulse welding were elucidated as processes which apply the principles of impact welding. Furthermore, a test rig was introduced which replicates the impact with the aim to make it easier to investigate. The functional principle of the test rig and special properties were discussed. Likewise, the experimental setup for electromagnetic pulse welding and its properties were presented.
Subsequently, the numerical simulation of both processes and the development of the models were introduced in detail. The electromagnetic calculation is a challenging aspect here. The evaluation of the numerical results alone shows that they are plausible. However, compared to the results of experimental investigations it was shown that significant deviations between simulation and experiment can still be observed. The prediction of the material flow at the high strain rates governing the impact does not represent the reality correctly.
Further works must not only include the improvement of the numerical representation of the mechanisms leading to the bond in the welded area but also macroscopic effects such as the material deformation under high strain rates.

10 Acknowledgements

The authors would like to thank the German Research Foundation (DFG) for gratefully funding the project which enabled this paper. Furthermore, the authors thank Baumüller, Dynamore, LSTC and PSTproducts for their support during the experimental and numerical works.

11 Literature

[1] Carpenter, S.H.; Wittman, R.H.: “Explosion Welding”, Annu. Rev. Mater. Sci., 1975.5:pp. 177-199
[2] Crossland, B.: “Explosive Welding of Metals and its Application”, Oxford University Press, Oxford, 1982, pp. 10-38
[3] Kashani, M.; Aizawa, T.: “Welding and Forming of Sheet Metals by Using Magnetic Pulse Welding (MPW) Technique”, 4th International Conference on High Speed Forming, 2010
[4] Turner, A.; Zhang, P.; Vohnout, V.; Daehn, G.: “Spot Impact Welding of Sheet Aluminum”, Materials Science Forum, Vols. 396-402, 2002, pp. 1573-1578
[5] Schäfer, R.; Pasquale, P.; Kallee, S.: “The Electromagnetic Pulse Technology (EMPT): Forming, Welding, Crimping and Cutting”, White Paper, http://pstproducts.com, 04-12-2015
[6] Schäfer, R.; Pasquale, P.: “Die Elektromagnetische Puls Technologie im industriellen Einsatz”, White Paper, http://pstproducts.com, 04-12-2015
[7] Winkler, R.: “Hochgeschwindigkeitsumformung”, VEB Verlag Technik, Berlin, 1973, pp. 22-74
[8] Pabst, C.; Groche, P.: “Electromagnetic Pulse Welding: Process Insights by High Speed Imaging and Numerical Simulation”, 6th International Conference on High Speed Forming, 2014
[9] Grignon, F.; Benson, D.; Vecchio, K.S.; Meyers, M.A.: “Explosive welding of aluminum to aluminum: analysis, computations and experiments”, International Journal of Impact Engineering 30, 2004, pp. 1333-1351
[10] Lysak, V.I.; Kuzmin, S.V.: “Lower boundary in metal explosive welding. Evolution of ideas”, Journal of Materials Processing Technology 212, 2012, pp. 150-156
[11] Groche, P.; Wagner, M.F.-X.; Pabst, C.; Sharafiev, S.: “Development of a novel test rig to investigate the fundamentals of impact welding”, Journal of Materials Processing Technology 204, 2014, pp. 2009-2017
[12] Kakizaki, S.; Watanabe, M.; Kumai, S.: “Simulation and Experimental Analysis of Metal Jet Emission and Weld Interface Morphology in Impact Welding”, Materials Transactions 52, 2011, pp. 1003-1008
[13] Wang, X.; Zheng, Y.; Liu, H.; Shen, Z.; Hu, Y.; Li, W.; Gao, Y.; Guo, C.: “Numerical study of the mechanism of explosive/impact welding using Smoothed Particle Hydrodynamics method”, Materials and Design 35, 2012, pp. 210-219
[14] Shribman, V.: “Magnetic Pulse Welding for Dissimilar and Similar Materials”, 3rd International Conference on High Speed Forming, 2008
[15] Göbel, G.; Kaspar, J.; Herrmannsdörfer, T.; Brenner, B.; Beyer, B.: “Insights into intermetallic phases on pulse welded dissimilar metal joints”, 4th International Conference on High Speed Forming, 2010

[16] Geyer, M.; Böhm, S.: “Influence of contact surface on weldability with electromagnetic pulses”, IIW Denver Annual Assembly, 2012
[17] Stern, A.; Shribman, V.; Ben-Artzy, A.; Aizenshtein, M.: “Interface Phenomena and Bonding Mechanism in Magnetic Pulse Welding”, Journal of Materials Engineering and Performance 23, 2014, pp. 3449-3458
[18] Song, J.; Kostka, A.; Veehmayer, M.; Raabe, D.: “Hierarchical microstructure of explosive joints: Example of titanium to steel cladding”, Materials Science and Engineering A 528, 2011, pp. 2641-2647
[19] Koschlig, M.; Veehmayer, M.; Raabe, D.: “Production of Steel-Light Metal Compounds with Explosive Metal Cladding”, 3rd International Conference on High Speed Forming, 2008
[20] Schäfer, R.; Pasquale, P.; Elsen, A.: “Material hybrid joining of sheet metals by electromagnetic pulse technology”, Key Engineering Materials 473, 2011, pp. 66-68
[21] Hisashi, S.; Isao, S.; Sherif, R.; Hidekazu, M.: “Numerical Study of Joining Process in Magnetic Pressure Seam Welding”, Transactions of JWRI 38, 2009, pp. 63-68
[22] Johnson, G.R.; Cook, W.H.: “A constitutive Model and Data for Metals subjected to large Strains, high Strain Rates and high Temperatures”, Proceedings of the 7th International Symposium on Ballistics 21, 1983, pp. 541-547
[23] Li, J.; Gao, H.; Cheng, G.J.: “Forming Limit and Fracture Mode of Microscale Laser Dynamic Forming”, Journal of Manufacturing Science and Engineering 12, 2010,